Picosecond dynamics of degenerate orthoexcitons in Cu_2O

D. W. Snoke* and J. P. Wolfe
Physics Department and Materials Research Laboratory, University of Illinois, Urbana, Illinois 61801
(Received 18 April 1990)

Previous time-resolved luminescence studies of orthoexcitons in Cu_2O have shown a "quantum saturation" behavior. Basically, it was found that for 10-ns laser pulses, which are comparable to the exciton lifetime, the exciton-gas temperature rises along the phase boundary for Bose-Einstein condensation as the density is increased. The microscopic processes that lead to such an unusual effect remained unresolved. To isolate the various kinetic processes, we have now conducted a study using 100-ps pulses, which are short compared with the orthoexciton lifetime. Combined with an increased time resolution, this short-pulse excitation has allowed us to observe some of the intrinsic rates of thermalization and decay of the orthoexcitons. At low-to-intermediate excitation levels, the decay of the gas temperature is found to agree with a model of acoustic-phonon emission, and the deduced exciton-phonon coupling is in basic agreement with that obtained from diffusion experiments. Another principal result is that the decay time of the gas temperature is significantly increased with increasing degeneracy, i.e., at high excitation level. After the short excitation pulse the orthoexcitons follow the Bose-Einstein phase boundary in density and temperature in a way similar to their behavior during the "steady-state" conditions of the long-pulse excitation. We conclude that the temperature rise is not simply due to insufficient thermalization caused by a shortening of the exciton lifetime; at high density there must be a heating mechanism such as Auger recombination.

I. INTRODUCTION

The semiconductor Cu_2O presents a beautiful opportunity to study the thermodynamics of an excitonic gas. Although it is a direct-gap semiconductor with spherical bands, the excitons in high-purity samples of Cu_2O have a long lifetime[1] due to the inversion symmetry that makes direct recombination forbidden to quadrupole order. The excitons (electron-hole pairs bound by Coulomb attraction) have relatively small radius (7 Å), high binding energy (150 meV), and a repulsive interaction,[2] which allows them to remain a nearly ideal gas up to high densities ($\sim 10^{20}$ cm^{-3}).

The luminescence of Cu_2O has been well studied since the 1950s.[3] Figure 1 shows a typical luminescence spectrum using cw excitation. The orthoexciton direct-recombination line (labeled X_0) appears at a photon energy 2.035 eV, the orthoexciton phonon-assisted replica involving the Γ_3^- optical phonon[4] occurs at photon energy 2.020 eV, and the only observed paraexciton replica, assisted by the Γ_5^- optical phonon, appears at 2.011 eV. Each of the phonon-assisted replicas has a shape given by $n(E) \propto D(E) f(E)$, where $D(E)$ is the excitonic density of states and $f(E)$ is the occupation number, which is simply $\exp(-E/k_B T)$ for a classical gas. Orthoexcitons are a triplet state analogous to spin 1; paraexcitons are a singlet state analogous to spin 0. Orthoexcitons have a short lifetime ($\tau < 10$ ns) due to their down conversion to paraexcitons. Paraexcitons have lifetimes approaching microseconds, due to the fact that their direct recombination is forbidden in Cu_2O.

Cu_2O has attracted interest lately because of its potential for demonstrating inherently quantum effects of Bose-Einstein statistics. The excitons are bosons under the condition[5] $na^3 \ll 1$, where a is the excitonic Bohr radius (7 Å) and n is the density. At $n = 10^{20}$ cm^{-3}, na^3 is still only 0.035. For a boson gas, the occupation number

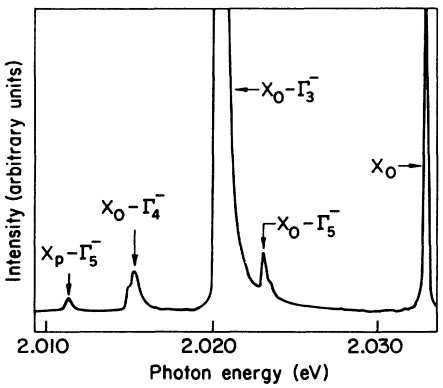

FIG. 1. The luminescence spectrum of Cu_2O taken at low excitation density and low temperature (2 K). The line labeled X_0 is the orthoexciton direct recombination; the phonon-assisted orthoexciton "replicas" are labeled by the symmetry of the optical-phonon involved. The direct paraexciton recombination, X_p, is strictly forbidden. "X_p-Γ_5" is the paraexciton phonon-assisted line, which is readily observable in cw experiments due to the long paraexciton lifetime. The ortho direct is cut off at about $\frac{1}{2}$ of its height; the Γ_3^- phonon-assisted ortho replica is cut off at about $\frac{1}{3}$ of its height.

is predicted to be

$$f(E)=1/\{\exp[(E-\mu)/k_BT]-1\} .$$

This occupation number leads to a line shape distinctly different from the classical line shape. It also leads to a critical density for Bose-Einstein condensation, given by $n_c=gCT^{3/2}$, where g is the exciton spin multiplicity and $C=2.612(mk_B/2\pi\hbar^2)^{3/2}$ is a constant depending only on exciton mass m and universal constants.

In a previous publication,[6] we reported the "quantum saturation" of orthoexcitons in Cu_2O. In those experiments, the orthoexciton density was increased from very low density to very high density ($\sim 10^{19}$ cm^{-3}) via excitation of the crystal surface with cavity-dumped Ar^+ laser pulses. The 10-ns pulse lengths are comparable to the orthoexciton lifetime. At the lowest densities, the excitonic temperature stayed near the lattice temperature (fixed by immersion in superfluid helium at 2 K), but when the orthoexciton density came within a factor of 2 of the critical density for Bose-Einstein condensation, the temperature increased as $n^{2/3}$, keeping the orthoexcitons "saturated" at the phase boundary for condensation over more than an order of magnitude in density variation. This behavior is shown as the solid dots in Fig. 2. The orthoexciton kinetic-energy spectrum, obtained from the phonon-assisted replica line shape, departs from the classical form and takes on the distinct Bose-Einstein shape but does not appear to have a significant condensate component.

More recently, we have reported[7] the *paraexciton* kinetic-energy spectrum, observed simultaneously with the orthoexciton spectrum. At intense excitation levels, the paraexciton spectrum displays a highly anomalous structure. We simultaneously observed rapid nondiffusive expansion of the excitons following their creation at the surface of Cu_2O. These spectroscopic and spatial data led us to conclude that the paraexcitons form a Bose condensate during the saturation of the orthoexcitons.

A major question has remained unanswered in the above work: Why does the excitonic temperature rise in the way it does with increasing density? Several possibilities come to mind: (1) The exciton lifetime is density dependent and becomes too short for the excitons to thermalize to the lattice within their lifetime; (2) the lattice itself is heated due to the high excitation levels; (3) an Auger two-body recombination process occurs, which both shortens the particle lifetime *and* increases the kinetic energy of the gas by producing an ionized plasma component; or (4) there is a quantum effect that favors an increase in temperature over Bose-Einstein condensation.

To address these issues, we have performed a series of experiments using shorter laser pulses (100 ps) and fast photon-counting time resolution (90 ps). In contrast to the "long" 10-ns pulse experiments, the gas is observed, for the most part, *after* the free carriers are injected by the 100-ps pulse; hence, the present experiments measure the relaxation of a highly excited system toward equilibrium. We have succeeded in estimating the acoustic-phonon emission rate and the cross section for Auger recombination and ionization. We have also found evidence for a time lag in the occupation of low-energy states, which could help to explain the saturation effect of the orthoexcitons.

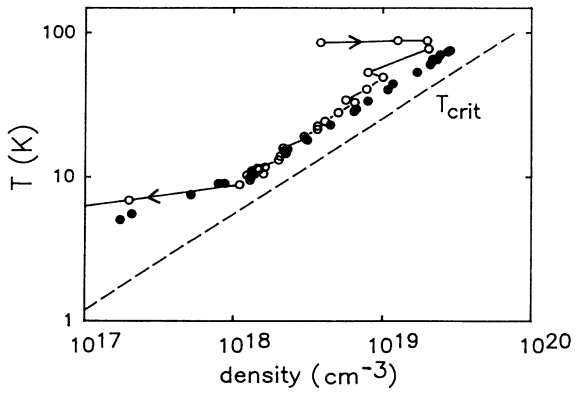

FIG. 2. The quantum saturation of the orthoexciton gas in Cu_2O, corresponding to a temperature rise with density, $T \propto n^{2/3}$. The solid circles are the temperatures and densities deduced from fits to the data from long (10-ns) excitation pulses in Ref. 6. The open circles are the fit temperatures and densities from the short-pulse (100-ps) data, as discussed in Sec. V of the text. The data points are connected by a line in order from earliest to latest—the arrows indicate increasing time delay. The dashed line is the critical density for Bose-Einstein condensation of orthoexcitons.

II. THERMALIZATION OF THE EXCITONIC GAS

Figure 3 shows the orthoexciton Γ_3^--phonon-assisted luminescence spectrum at various times during and after a high-power, 100-ps mode-locked, cavity-dumped Ar^+ laser pulse ($h\nu=2.41$ eV). The laser is focused to a spot about 20 μm in diameter, producing an incident power density of about 10^8 W/cm^2. The photoluminescence is selected with a 1-m spectrometer (typical resolution 0.5 Å) and detected with a Hamamatsu multichannel plate phototube with 90-ps resolution (the full width at half maximum measured with a 6-ps calibration pulse). Time "$t=0$" is defined here as the time when the detected laser signal reaches about 3% of its maximum and corresponds to the maximum of the measured gas temperature. The time-resolved spectra show the cooling of the excitonic gas after its creation with large excess energy ($h\nu > E_{gap} \approx 0.375$ eV).

Figure 4 shows a similar series of spectra for a much lower power density, obtained by defocusing the laser spot to about 2 mm. The width of a given spectrum roughly corresponds to the temperature of the gas at that instant. These spectra indicate a cooling of the gas that is much more rapid than in the case of the high-intensity laser pulse.

Figure 5 shows the effective temperature associated with the high-energy tail, taken from the best straight line fit to the spectra on a semilog plot. (For example, see Figure 8 below.) Specifically, $k_BT_{eff}=-I/(dI/dE)$.

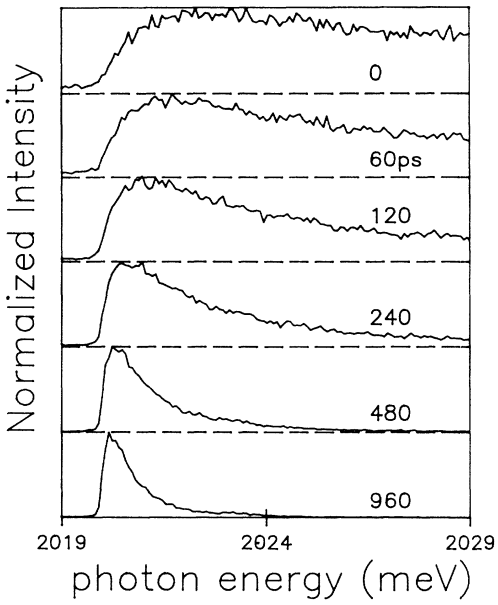

FIG. 3. The X_0-Γ_3^- luminescence spectrum of the orthoexcitons at various times during and after a *high*-power, 100-ps Ar^+ laser pulse. Pulse energy is approximately 20 nJ, laser spot size is approximately 20 μm. Spectra are normalized to the same height; relative intensities are plotted in Fig. 9.

In the case of Boltzmann statistics with $I \propto E^{1/2}\exp(-E/k_BT)$, the high-energy limit of $-I/(dI/dE)$ is exactly k_BT. In the low-intensity case shown, the temperature initially approaches the lattice temperature with a lifetime of less than 100 ps, close to the limit of our temporal resolution, and the rate slows as the gas energy decreases.

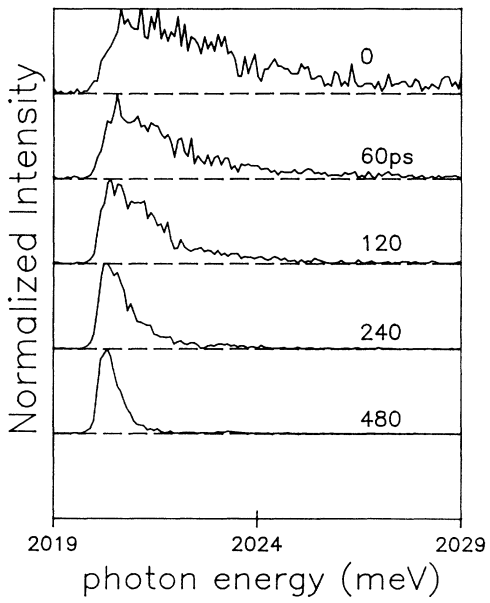

FIG. 4. The X_0-Γ_3^- luminescence spectrum of the orthoexcitons at various times during and after a *low*-power, 100-ps Ar^+ laser pulse. The gas thermalizes to the lattice temperature much more quickly than in the high-power case of Fig. 3. Pulse energy is approximately 20 nJ, laser spot size is approximately 2 mm.

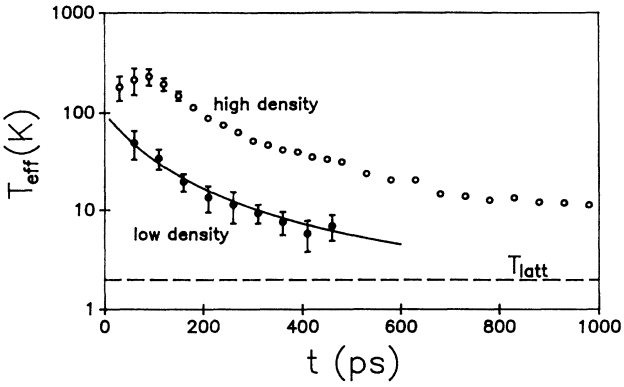

FIG. 5. The effective temperature as a function of time for the two cases of Figs. 3 and 4. The temperature is obtained from the spectra by the method discussed in the text. The solid line in the low-density case is the calculated fall in temperature due to acoustic-phonon emission, as discussed in the text.

These low-power thermalization data provide an estimate of the acoustic-phonon emission rate for the excitons. According to deformation-potential theory, the rate of energy loss by acoustic-phonon emission should be proportional to $T^{3/2}$. Specifically, if the theory for electrons is generalized to apply to excitons, the rate of energy loss per particle is[8]

$$\Gamma_{ac}=2.03\frac{\Xi^2 m^{5/2}}{\hbar^4\rho}(k_BT)^{3/2}(1-T_{latt}/T)\ , \tag{1a}$$

where Ξ is the deformation potential, m is the exciton mass, ρ is the mass density of the crystal, T is the exciton temperature, and T_{latt} is the lattice temperature. Using $m=2.7m_0$ for the mass,[9] and $\Xi=1$–2 eV, obtained from pressure measurements[10] and mobility measurements,[11] this gives

$$\Gamma_{ac}=0.2\text{–}0.8(\text{meV/ns}\,K^{3/2})T^{1/2}(T-T_{latt}). \tag{1b}$$

At $T=100$ K, this gives a thermalization time of 10–50 ps. The higher value is consistent with the thermalization rate at low excitation power seen in Fig. 5.

To be more quantitative, we have modeled the temperature as a function of time using formula (1). The change in temperature dT per time step dt is $dT=\Gamma_{ac}(T)dt/k_B$; thus $T(t)$ for a given value of Γ_{ac} can be found by numerical iteration. The solid curve in Fig. 5 shows the results of this model for a gas starting at $T=100$ K and falling to a lattice temperature of 2 K, with the coefficient in Eq. (1b) equal to 0.2 meV/ns $K^{3/2}$, the lower limit of the above calculation, indicating $\Xi\simeq 1$ eV for excitons, in agreement with Ref. 11.

We now concentrate on the "anomalous" rise in excitonic gas temperature observed at high excitation level. Do the elevated temperatures in the high-intensity case come about because of heating of the lattice? The local lattice temperature can be estimated from the shift of the exciton line. The band gap of Cu_2O is known[1] to vary roughly as E_0-bT^2, where $b\simeq 0.0015$ meV/K.[2] As seen in Figs. 3 and 4, the low-energy edge varies less than 0.1

meV, implying $T_{\text{latt}} < 15$ K. This was true for the previously published cavity-dumped Ar^+ data, as well.[6,7]

This lack of a significant lattice heating is consistent with the total energy of the laser pulse deposited in the lattice. Each 100-ps pulse has about 0.01 μJ energy at 5145 Å, corresponding to 3×10^{10} photons, each with 0.375 eV excess energy, resulting in about 4×10^{-10} cal delivered to the lattice. The heat capacity of Cu_2O is roughly 1.4×10^{-6} cal/g K $(T/K)^3$ at low temperature,[12] and the volume of the excitation region is about 2×10^{-8} cm^3, yielding a lattice temperature rise of less than 10 K. Diffusion of heat away from the excitation region will reduce this temperature.

For the excitons to establish a temperature well above the lattice temperature, the interaction time of the excitons among themselves must be short compared to the acoustic-phonon emission time. How high must the gas density be to establish such a quasiequilibrium? As seen above, the phonon emission time is less than 50 ps at 100 K. Estimating the exciton-exciton scattering time as $1/n\sigma v$, where n is the density, v is the average thermal velocity, and σ is the scattering cross section, this gives the constraint on the scattering length $l=(n\sigma)^{-1}<2\times10^4$ cm. For $\sigma=\pi a^2$, with $a=7$ Å, the excitonic Bohr radius, this implies $n>3\times10^{17}$ cm^{-3}. As discussed in Sec. IV. The densities determined from spectral fits to the Bose-Einstein distribution clearly meet this condition. Thermalization times are also affected by scattering with optical phonons.

The results shown in Fig. 5 give us an important insight into the quantum saturation behavior of the orthoexcitation gas, which was reported earlier for steady-state conditions produced by longer (10-ns) pulses.[6] The reduction in the decay rate of the gas temperature at high density shown in Fig. 5 implies that the steady-state temperature rise near the phase boundary for Bose-Einstein condensation is not simply due to insufficient thermalization caused by a shortening of the exciton lifetime. There must be an additional heating process in the gas of excitons at high density. We now examine one effect that may lead to this heating.[13]

III. AUGER RECOMBINATION EFFECT

Figure 6 shows the orthoexciton decay rate extracted from the temporal change in total luminescence intensity of the data of Fig. 4, at times greater than 300 ps, long after any generation by the exciting laser pulse. The vertical axis gives the fractional rate of change in total phonon-assisted orthoexciton luminescence intensity; the horizontal axis gives the total intensity, multiplied by a constant to calibrate it to density. This assumes a constant gas volume during the first nanosecond. This assumption is seen to be reasonable in Sec. V, based on the estimation of density from spectral fits.

As seen in Fig. 6, the decay rate is roughly linear with density; the slope is 0.8. A linear dependence is expected for a two-body collision-dependent recombination mechanism.[14] We can roughly estimate the cross section for such a process assuming classical statistics. The rate of recombination is $\Gamma_A=\sigma_A n v$, where n is the orthoexciton density and $v=(3k_BT/m)^{1/2}$ is the average velocity. Setting n equal to the orthoexciton density and Γ_A equal to the measured decay rate gives a cross section for recombination $\sigma_A\simeq8$ Å^2, assuming an average temperature of 20 K during the decay. The two-body recombination mechanism likely depends on the total exciton density, however, and not merely on the orthoexciton density. As shown previously with long pulses,[7] the paraexciton population is comparable to that of the orthoexciton. In the density range of interest here, the paraexciton density is expected to be 1–3 times the orthoexciton density. Using this range of total densities in the above formula gives a cross section $\sigma_A=2$–4 Å^2.

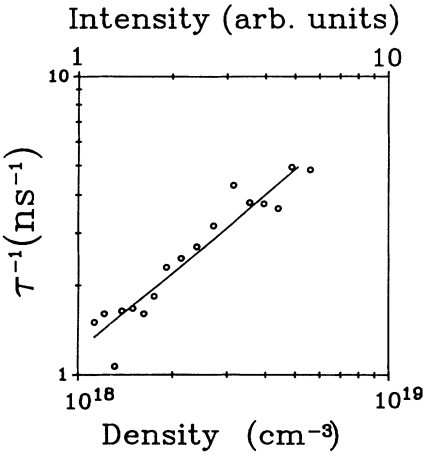

FIG. 6. The decay rate of the orthoexcitons as a function of their total intensity during a single decay cycle, from the same data as Fig. 3. The decay rate is found by the instantaneous change in the luminescence intensity, i.e., $\tau_x^{-1}=dI/Idt$. On the lower axis, the intensity is converted to density by an overall multiplicative factor. The exciton gas density scale is calibrated by comparison to the density deduced from spectral fits as shown in Fig. 8(a). The solid line shows the best fit to a straight line, which has a slope of 0.8.

The observed rate is the sum of the two-body decay rate plus all one-body orthoexciton decay rates. The orthoexcitons can decay into paraexcitons via an intrinsic single-phonon emission process[15] that has rate[16] $\Gamma_{\text{op}}\simeq0.3\times10^8$ $(\text{ns}^{-1}\text{K}^{3/2})T^{3/2}$. Because of the $T\propto n^{2/3}$ "saturation" observed in the orthoexciton gas, the $T^{3/2}$ dependence of the single-phonon down-conversion process also implies a decay rate of the orthoexcitons that is linear with density. The above value for Γ_{op}, from Ref. 16, is comparable to the decay rates measured here for the exciton temperatures, e.g., a lifetime of about 200 ps at 30 K. The exciton temperatures in Ref. 16 were equal to the lattice temperature, however. If the exciton temperature rises but the lattice temperature remains near 2 K, the model of Ref. 15 predicts that the intrinsic lifetime should be three times longer, or 600 ps at 30 K. It therefore seems likely that the orthoexciton decay rate reported here includes a two-body term with cross section ~2 Å, as well. The orthoexcitons also decay by radiative recombination and nonradiative recombination at impurities, which are probably much slower processes in these high-purity samples.

One possible type of two-body decay process is an Auger process, suggested by Mysyrowicz, Hulin, and Benoit a la Guillaume.[17] In this process, two excitons collide and one recombines, giving its gap energy to the other, which ionizes. Another possible process, suggested by Mysyrowicz,[18] is a collision-induced spin flip of two orthoexcitons to become two paraexcitons, which lie 12 meV lower by an exchange splitting. Both of these processes predict orthoexciton lifetimes inversely proportional to their density; however, the spin-flip process does not lead to conversion of paraexcitons up to orthoexcitons, whereas the ionized carriers produced by the Auger process reform into both orthoexcitons and paraexcitons. Direct evidence for an Auger process is found in cw experiments where the long-lived paraexciton species is dominant. In that case, an anomalously high population of orthoexcitons is observed,[19] whose intensity increases as the square root of the paraexciton population, as expected for an Auger generation of orthoexcitons.

The Auger process leads to a heating of the exciton gas at high density because the ionized carriers can lose their energy not only to phonons but also to the exciton gas via collisions.[18] We have modeled the dependence of the gas density and temperature on excitation power, incorporating an Auger process, phonon-assisted, ortho-to-para conversion, and optical- and acoustic-phonon emission. The acoustic-phonon cooling rate measured by this work is used. This model shows that an Auger process, with a rate of about that estimated here, can explain the temperature rise up to about 30 K. Above this temperature, however, optical-phonon emission should produce a significant cooling, which is not apparent in the data. These results are planned for publication in another paper.

IV. BOSE-EINSTEIN ENERGY DISTRIBUTION

Figure 7 shows three time-resolved orthoexciton spectra, as in Fig. 3, but plotted logarithmically. The spectra are fit to an ideal Bose-Einstein distribution

$$n(E)=D(E)f(E)\propto E^{1/2}/\{\exp[(E-\mu)/k_BT)]-1\},$$

drawn as the dashed lines. The fits are quite satisfactory except for the significant luminescence present at $E<0$, i.e., a low-energy tail. As we previously found,[7] this tail can be mainly accounted for with a Lorentzian broadening of the spectrum. Also, the luminescence spectrum is expected to represent a range of gas densities and temperatures. A continuous variation of density and temperature is found to give a luminescence spectrum that is very similar to that of a homogeneous Bose-Einstein gas with single (average) density and temperature.[7] The fits here to a spectrum with single μ and T are quite successful.

Figure 8 contains the time evolution of μ and T obtained from fitting the data of Fig. 3 to the simple Bose-Einstein distribution $n(E)$. Also plotted as a function of time is the density deduced from the fitted μ and T values via the formula $N=\int D(E)f(E)dE$. The density deduced from the fits follows closely the total luminescence intensity data, plotted as the open circles in Fig. 8(a). The agreement implies that the volume of the observed region of gas does not change significantly during the time of thermalization, i.e., about 1 ns.

The chemical potential μ, plotted in Fig. 8(c), saturates at about $-0.2k_BT$. The gas remains saturated at this value beyond a nanosecond, at which time the intensity becomes too low for good fits. This quantum saturation behavior was also found in the experiments using 10-ns cavity-dumped pulses.[6] The open circles in Fig. 2 show the fit temperature and density for the short-pulse data of Fig. 8. The arrows indicate the direction of time in the short-pulse experiment. As seen, the behavior closely follows the quasi-steady-state, long-pulse case, except early in the pulse when the gas has not yet cooled to reach the

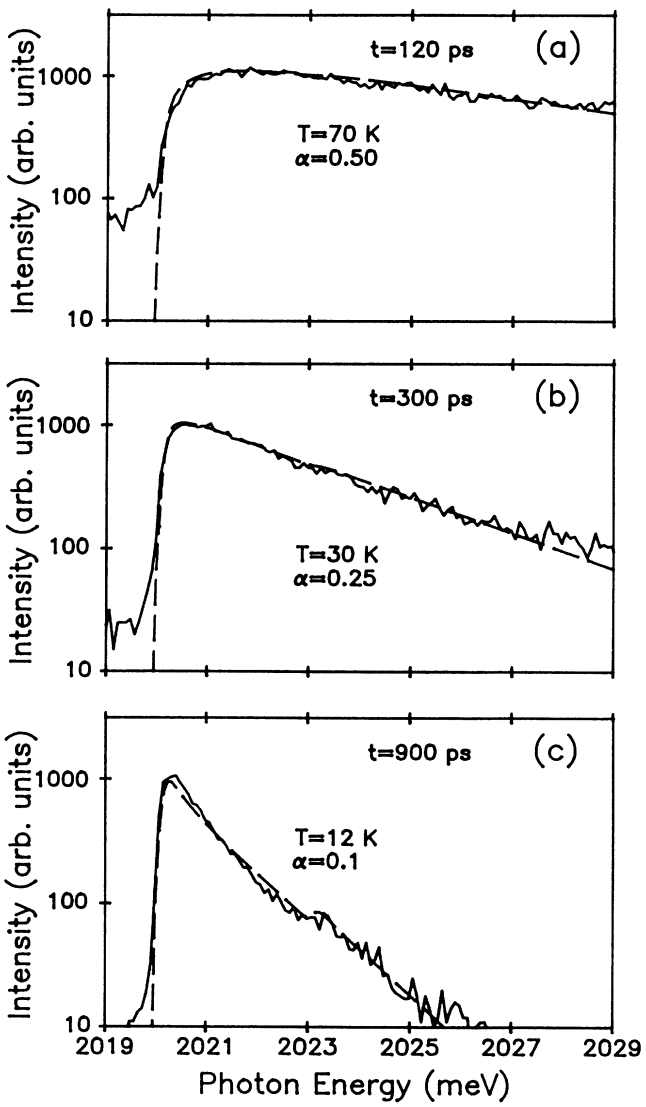

FIG. 7. The orthoexciton luminescence spectra from the data of Fig. 3, plotted semilogarithmically at three times, fit to the ideal Bose-Einstein distribution $n(E)=f(E)D(E)$. The dashed lines are the best fit in each case, with the values of T and $\alpha=-\mu/k_BT$ shown. The two parameters are nearly orthogonal; the value of T is constrained by the straight-line fit to the high-energy tail. The fitted spectrum in each case is convolved with a triangle function of width 0.5 Å to take into account the spectrometer resolution.

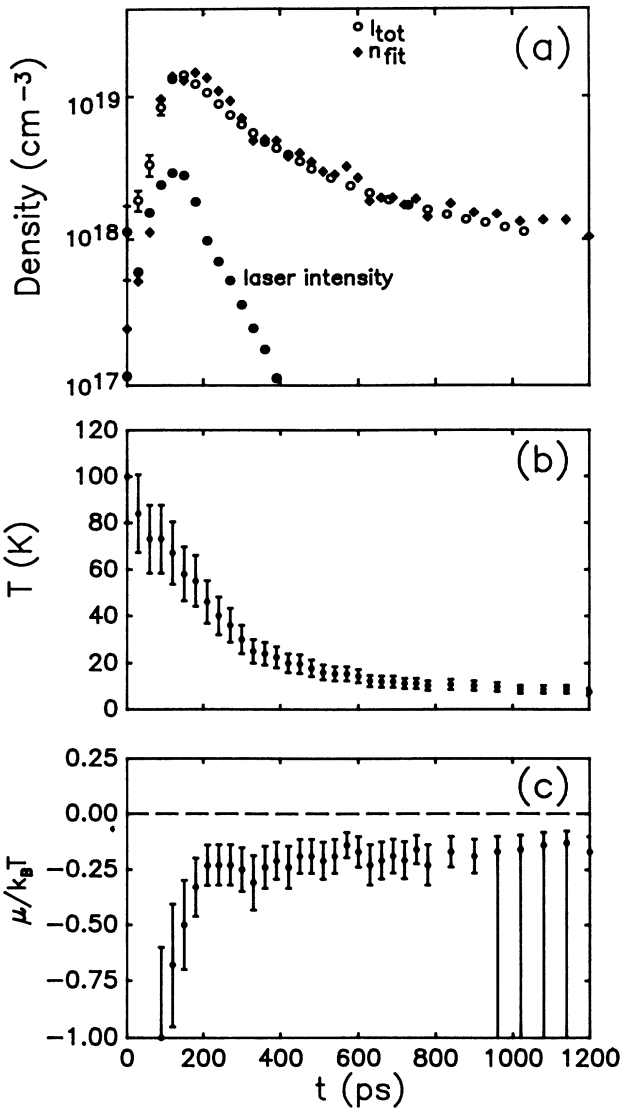

FIG. 8. The thermodynamic parameters of the gas as deduced from the spectral fits to the data of Fig. 3. The density n_{fit} in (a) is obtained from the fitted values of T and μ shown in parts (b) and (c). As seen in part (a), there is a strong correlation between the fit density and the total phonon-assisted orthoexciton luminescence intensity.

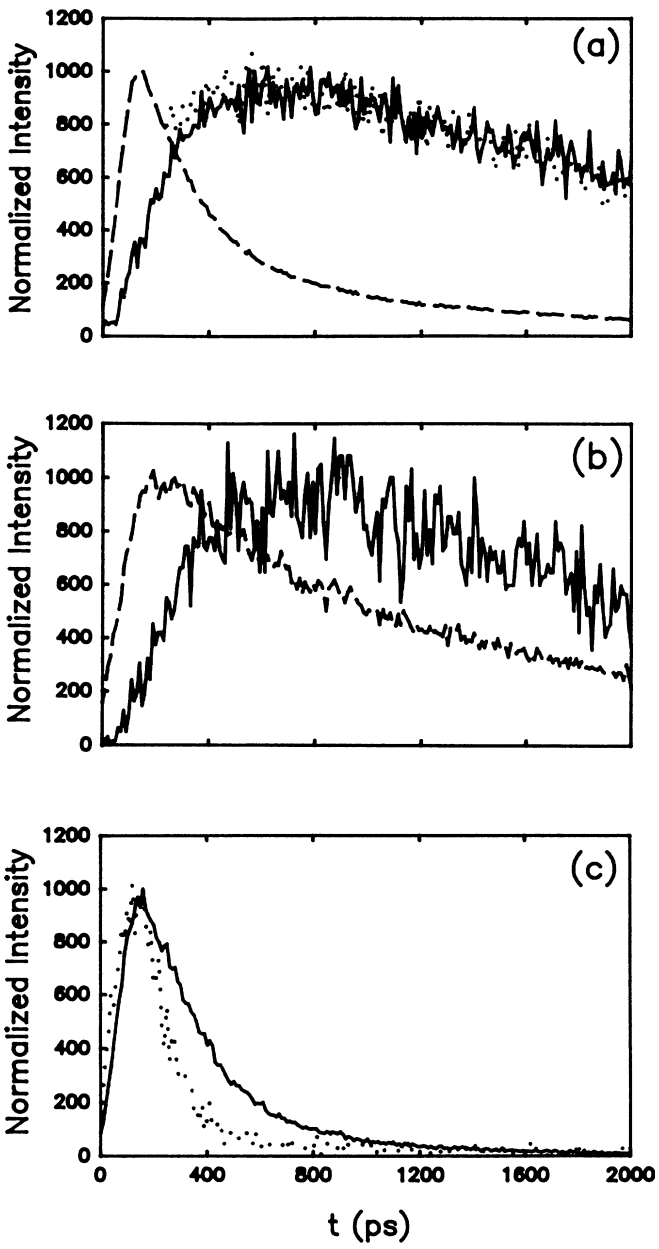

FIG. 9. (a) Dashed line: The total phonon-assisted orthoexciton luminescence intensity as a function of time, for the *high*-density data of Fig. 3. Solid line: The intensity of the low-energy tail ($2.018 < E_{photon} < 2.020$ eV) of the phonon-assisted luminescence. Small dots: The total intensity of the orthoexciton direct-recombination line as a function of time. All three curves are normalized to the same peak intensity. The latter two correlate with each other in time in showing a delay in reaching their peak. (b) Dashed line: The total phonon-assisted orthoexciton luminescence intensity as a function of time, for the *low*-density data of Fig. 4. Solid line: The intensity of the low-energy tail ($2.018 < E_{photon} < 2.020$ eV) of the phonon-assisted luminescence. A time delay to the peak intensity from low-kinetic-energy states is also seen in the low density data. (c) Solid curve: Phonon-assisted luminescence at exciton kinetic energy 2.9 meV, for the high-density data of Fig. 3. Small dots: The low-intensity data of Fig. 4 at the same exciton kinetic energy.

phase boundary.

The fact that the gas shows the same saturation behavior as in the long-pulse case, even well after the short laser pulse, clearly indicates that the Bose-Einstein shape of the orthoexciton energy distribution seen in quasi-steady-state conditions with long-pulse excitation[6,7] does not depend fundamentally on the presence of the laser field. Instead, it depends only on the total exciton density at a given point in time.

V. LOW-ENERGY STATE FILLING

The scattering of particles into low-energy states including the ground state is critical for Bose-Einstein condensation. We therefore examine more closely the popu-

lation of these states.

Figure 9(a) shows a comparison of the temporal behavior of three selections of the orthoexciton luminescence, for the *high*-intensity excitation data of Fig. 3. The dashed line is the total orthoexciton phonon-assisted luminescence intensity, which is proportional to the total number of orthoexcitons. The small dots are the total orthoexciton direct-recombination intensity, and the solid line is the luminescence from the low-energy tail ($2.018 < E_{\text{photon}} < 2.020$ eV) of the phonon-assisted orthoexciton line. The orthoexciton direct-recombination intensity is not plotted before $t = -300$ ps because it is obscured by the high-temperature tail of the phonon-assisted line. As seen in this figure, the direct-recombination intensity shows the same temporal behavior as the intensity of the low-energy exciton luminescence. This is not surprising, since the no-phonon direct recombination line only samples low-energy states ($k \simeq k_{\text{photon}}$) due to momentum conservation. The interesting result, however, is the time lag between the peak in total luminescence and the peak of the low-energy luminescence, roughly 0.6 ns. Basically, these data indicate that significant time is required for the gas to relax into low-energy states. A similar time lag between the peak of the phonon-assisted luminescence and the peak of the direct-recombination luminescence also occurs in the long-pulse case.[7]

Figure 9(b) shows a similar comparison for the *low*-intensity excitation data of Fig. 4. The dashed line is the total orthoexciton phonon-assisted luminescence intensity and the solid line is the luminescence from the low-energy tail of the phonon-assisted orthoexciton line. The low-energy states in this case show almost the same time lag in filling as in the high-density case, about 0.8 ns. On the other hand, the population of high-kinetic-energy states decays more rapidly in the low-intensity case, corresponding to a quicker thermalization, as discussed in Sec. II. Figure 9(c) shows a comparison of the temporal behavior of the phonon-assisted luminescence intensity obtained by sampling a higher kinetic energy, for both the high- and low-intensity cases.

The population of the low-energy states is directly related to the temperature of the gas. If the gas were simply classical with a Boltzmann occupation $\exp(-E/k_B T)$, then the fraction of particles in a spectral region dE near $E=0$ would be equal to

$$f = (dE)^{1/2}\exp(-dE/k_B T)dE \Big/ \int_0^\infty E^{1/2}\exp(-E/k_B T)dE \propto 1/T^{3/2} . \quad (2)$$

In other words, the intensity of luminescence from low-energy states at a given time is expected to be proportional to $I_{\text{tot}}/T^{3/2}$, where I_{tot} is the total exciton luminescence intensity. The fact that the total number of particles in low-energy states has nearly the same temporal behavior for both the high and low excitation level in Fig. 9 is therefore an interesting coincidence, considering the different time dependences, $I_{\text{tot}}(t)$ and $T(t)$ in these two cases. The overall orthoexciton intensity $I_{\text{tot}}(t)$ falls much faster in the high density case, but the temperature falls much more slowly, suppressing the number in low-energy states until late times.

While the high gas temperatures at high density tend to suppress the number of particles in low-energy states, the increased quantum degeneracy at high density tends to increase the fraction of excitons having energy near the ground state. In the following, we attempt to quantify these effects of temperature and quantum statistics on the number of particles in low-energy states.

The solid lines in Fig. 10 show the ratio of the low-energy orthoexciton intensity, I_0, divided by the total orthoexciton phonon-assisted intensity, I_{tot}, as a function of time. The "high-power" curve corresponds to the data of Fig. 9(a), smoothed considerably, and the "low-power" curve corresponds to the data of Fig. 9(b), also smoothed. The dashed line in each case is $1/T^{3/2}$, the classical low-energy fraction from Eq. (2), using the spectral fit temperatures. This is multiplied by a constant to equal I_0/I_{tot} at late times, because at $t \simeq 2$ ns the energy distribution is Maxwell-Boltzmann in both cases.

In the high-power case, the actual low-energy occupation is about a factor of 2 above the classical expectation during the whole time the gas is saturated near the Bose-Einstein condensation phase boundary. This factor of 2 corresponds to $\alpha = 0.2$ for an ideal boson gas, as shown in the theoretical calculation of Fig. 11. This value of α is in rough agreement with the saturation value of α in Fig. 8(c). In the low-power case, the gas is also initially saturated at the Bose-Einstein phase boundary but becomes

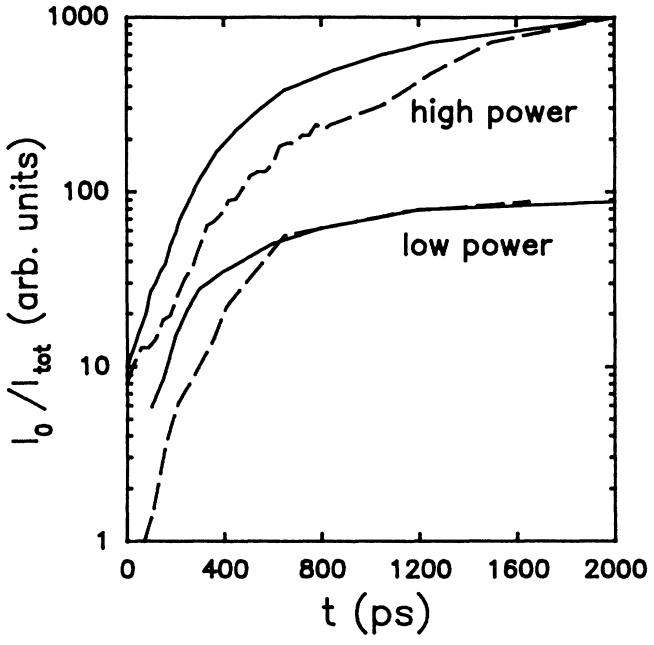

FIG. 10. Solid lines: The ratio of I_0, the intensity of luminescence from low-energy states ($2.018 < E_{\text{photon}} < 2.020$ eV), to I, the total phonon-assisted luminescence intensity, as a function of time for the two cases shown in Fig. 9(a) (high power) and Fig. 9(b) (low power). Dashed lines: $A/T^{3/2}$ in each case, where T is the spectral fit temperature and A is a constant fixed by equating $A/T^{3/2}$ to I_0/I at $t=2$ ns in each case. For Maxwell-Boltzmann statistics, I_0/I is proportional to $1/T^{3/2}$.

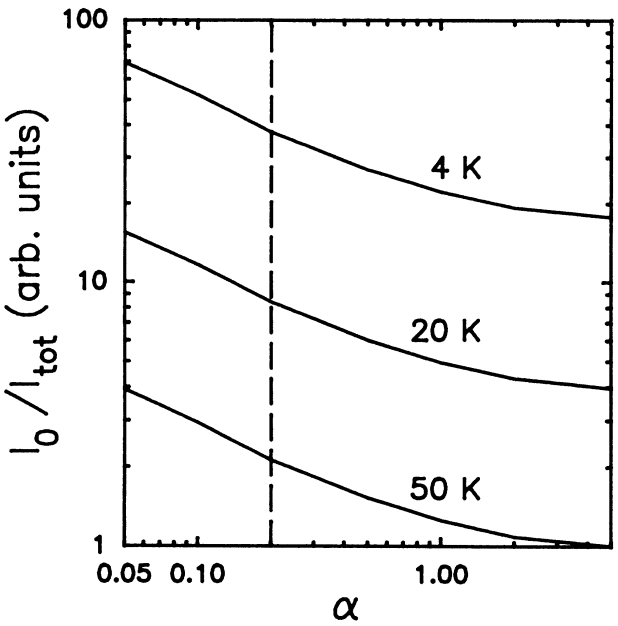

FIG. 11. The ratio of the population of low-energy states to total population as a function of normalized chemical potential, $\alpha=-\mu/k_BT$, for three temperatures. The function plotted is $g(\mu,T)=[(dE)^{3/2}/(e^{(dE-\mu)/kT}-1]/\int[dEE^{1/2}/(e^{(E-\mu)/kT)}-1]$. The dashed line at $\alpha=0.2$ corresponds to an enhancement of the ratio I_0/I_{tot} by about a factor of 2, which correlates the data of Figs. 10 and 8(c).

classical much sooner.

This analysis of the low-energy population supports the conclusions drawn from the spectral fits in Sec. IV, that the orthoexciton gas quickly establishes a quasiequilibrium temperature and chemical potential in the quantum degenerate regime, very near to Bose-Einstein condensation. A similar analysis using the population of low-energy states to check the quantum statistics was reported in Ref. 6.

VI. CONCLUSION

The two principal results of this study involve the cooling of the exciton gas following its creation with large kinetic energy. First, at low excitation power, the decay of the gas temperature—as determined from the high-energy tail of the luminescence spectrum—follows the expectation for acoustic-phonon emission. Second, at high excitation level, the rate of cooling is markedly slower.

A slower cooling rate at high density may come about in part because of collision processes (e.g., Auger recombination and/or possibly ortho-para conversion) that raise the kinetic energy of the gas. Further evidence for a two-body recombination process is the nearly linear dependence of the orthoexciton lifetime on the gas density.

Another striking observation is the quantum saturation effect. For times up to a nanosecond following the laser pulse, the ideal Bose-Einstein distribution fits the spectra well. During its relaxation after a short pulse, the gas exhibits a saturation at the Bose-Einstein-condensation phase boundary, as was previously seen in near steady-state conditions with longer excitation pulses. A strong correlation of the fitted density values and the luminescence intensity indicates that little volume expansion occurs, at least at early times, in contrast to the fast expansion observed at $t>10$ ns in the long-pulse experiments.

Observation of the time-dependent population of states with low kinetic energy also shows the quantum saturation effect. Within our measurement resolution of about 100 ps, the gas quickly establishes a quasiequilibrium temperature and chemical potential governed by the quantum statistics of a nearly ideal gas. Comparison of spectral fit temperature and the low-kinetic-energy population indicates that at high density the gas remains saturated at $\alpha\simeq 0.2$ up to about 1.4 ns.

The unusual kinetics of the orthoexcitons are inherently related to the kinetics of the paraexcitons.[7] The two-component nature of the exciton gas is the subject of further experiments and theoretical modeling.

ACKNOWLEDGMENTS

This work has been supported by the National Science Foundation under Grant No. DMR87-22761. Facility support has been provided by Materials Research Laboratory Grant No. DMR86-12860. We thank P. J. Dunn of the Smithsonian Institute for providing a natural, high-purity Cu_2O sample. We thank D. Wake for the use of a synch-pumped dye laser and L. Faulkner for the loan of photon counting equipment. A. Mysyrowicz has provided valuable advice and suggestions.

---

*Present address: Max-Planck-Institut für Festkörperforschung, Heisenbergstrasse 1, 7000 Stuttgart 80, Federal Republic of Germany.

[1]A. Mysyrowicz, D. Hulin, and A. Antonetti, Phys. Rev. Lett. **43**, 1123 (1979); **43**, 1275E(E) (1979).

[2]See F. Bassani and M. Rovere, Solid State Commun. **19**, 887 (1976). A. I. Bobrysheva and S. A. Moskalenko, in Phys. Status Solidi B **119**, 141 (1983), calculate that the interaction is repulsive in general except between two orthoexcitons with summed spin $s=0$, which can form a biexciton with binding energy ~ 0.7 meV. No biexcitons have been observed in Cu_2O.

[3]For a review of Cu_2O properties see V. T. Agekyan, Phys. Status Solidi A **43**, 11 (1977).

[4]We use the O_h symmetry notation convention here given by Γ_1, Γ_2, Γ_3, Γ_4, and Γ_5 equal to Γ_1, Γ_2, Γ_{12}, Γ_{15}, and Γ_{25}, respectively.

[5]For a review of the boson properties of excitons see E. Hanamura and H. Haug, Phys. Rep. **33**, 209 (1977).

[6]D. W. Snoke, J. P. Wolfe, and A. Mysyrowicz, Phys. Rev. Lett.

59, 827 (1987).

[7]D. W. Snoke, J. P. Wolfe, and A. Mysyrowicz, Phys. Rev. Lett. **64**, 2543 (1990); Phys. Rev. B **41**, 11 171 (1990); A. Mysyrowicz, D. W. Snoke, and J. P. Wolfe, Phys. Status Solidi B **159**, 387 (1990).

[8]E. M. Conwell, Solid State Phys. Suppl. **9**, 122, (1967).

[9]N. Caswell, J. S. Weiner, and P. Y. Yu, Solid State Commun. **40**, 843 (1981).

[10]H.-R. Trebin, H. Z. Cummins, and J. L. Birman, Phys. Rev. B **23**, 597 (1981); K. Reimann and K. Syassen, Phys. Rev. B **39**, 11 113 (1989).

[11]D. P. Trauernicht and J. P. Wolfe, Phys. Rev. B **33**, 8506 (1986).

[12]L. V. Gregor, J. Phys. Chem. **66**, 1645 (1962).

[13]Heating of photexcited carriers for high optical and current excitation has previously been reported for GaAs quantum-well structures. In those cases, two mechanisms were considered to explain the reduction in carrier cooling: screening of the carrier–LO-phonon interaction and nonequilibrium populations of optical phonons. We do not consider those processes here, but we note that the Auger process for carriers in an electron-hole plasma in GaAs is a three-body process, and the small phase space for final states of the single remaining particle makes this process rather weak. Indeed, the carrier heating at high density in GaAs is accompanied by a longer carrier lifetime. In the case of Cu_2O, the lifetime shortens at high density, consistent with a dominant Auger process. The final state for an Auger recombination of excitons, involving two hot carriers, would seem to make this process much more likely than the three-body process in GaAs. For GaAs quantum-well carrier cooling, see, for example, K. Kash, J. Shah, D. Block, A. C. Gossard, and W. Wiegmann, Physica B **134**, 189 (1985), and J. F. Ryan, *ibid.* **134**, 403 (1985). For theory of nonequilibrium optical phonons in these structures, see, for example, P. Kocevar, *ibid.* **134**, 155 (1985), and P. J. Price, *ibid.* **134**, 164 (1985).

[14]From classical scattering theory, the rate should actually be $\Gamma_A \propto nT^{1/2}$, which in the orthoexciton $n \propto T^{3/2}$ saturation regime leads to the expectation $\Gamma_A \propto n^{4/3}$.

[15]D. W. Snoke, J. P. Wolfe, and D. P. Trauernicht, Phys. Rev. B **41**, 5266 (1990).

[16]J. S. Weiner, N. Caswell, P. Y. Yu, and A. Mysyrowicz, Solid State Commun. **46**, 105 (1983).

[17]A. Mysyrowicz, D. Hulin, and C. Benoit a la Guillaume, J. Lumin. **24/25**, 629 (1981).

[18]A. Mysyrowicz (private communication).

[19]D. P. Trauernicht and J. P. Wolfe, Phys. Rev. B **34**, 2561 (1986).